arXiv:1609.03707v1 [cond-mat.mes-hall] 13 Sep 2016

Efficiency bounds on thermoelectric transport in magnetic fields: The role of inelastic processes

Kaoru Yamamoto,[1] Ora Entin-Wohlman,[2,3] Amnon Aharony,[2,3] and Naomichi Hatano[4]

[1]*Department of Physics, The University of Tokyo, Komaba 4-6-1, Meguro, Tokyo 153-8505, Japan* *
[2]*Raymond and Beverly Sackler School of Physics and Astronomy, Tel Aviv University, Tel Aviv 69978, Israel*
[3]*Physics Department, Ben Gurion University, Beer Sheva 84105, Israel*†
[4]*Institute of Industrial Science, The University of Tokyo, Komaba 4-6-1, Meguro, Tokyo 153-8505, Japan*‡

(Dated: September 14, 2016)

We examine the efficiency of an effective two-terminal thermoelectric device under broken time-reversal symmetry. The setup is derived from a three-terminal thermoelectric device comprising a thermal terminal and two electronic contacts, under a magnetic field. We find that breaking time-reversal symmetry in the presence of the inelastic electron-phonon processes can significantly enhance the figure of merit for delivering electric power by supplying heat from a phonon bath, beyond the one for producing the electric power by investing thermal power from the electronic heat current. The efficiency of such a device is bounded by the non-negativity of the entropy production of the original three-terminal junction. The efficiency at maximal power can be quite close to the Carnot efficiency, but then the electric power vanishes.

PACS numbers: 72.15.Jf,72.20.Pa,84.60.Rb,05.70.Ln

Achieving high efficiencies in thermoelectric nanodevices is one of the main goals of contemporary research on nanostructural materials and setups [1–3]. It is well known that the efficiency (the ratio of the output power to the invested one) of a heat engine operating between two reservoirs is bounded by the Carnot efficiency. This extreme efficiency is reached in a quasi-static process which lasts for an infinite time and therefore the extracted power vanishes. The maximal efficiency that can be achieved by a heat engine delivering a finite electric power in a two-terminal geometry is usually expressed in terms of a single material- and setup-dependent parameter, called the figure of merit, ζ. The larger the ζ, the higher the maximal attainable efficiency can be. The possibility to significantly enhance ζ of a nanostructure, and even to reach the limit of reversibility by exploiting transmission resonances, has been extensively discussed [4–6]; the maximal efficiency attained at finite output powers [7] has been explored along similar lines. A recent theoretical endeavor introduced the concept of stochastic efficiencies, pertaining to strong fluctuations in the efficiency of small systems (see, e.g., Refs. 8–11). The bound on this efficiency depends on the protocol by which the long-time limit is reached.

Another promising route of research is the multi-terminal nanoscale heat engines [12, 13], e.g., those built on coupled quantum dots [14, 15]. In contrast to the two-terminal geometry, where heat and charge are carried by the same particles, it is possible in the three-terminal setups to spatially separate the heat reservoir from the current circuit [14, 16], thus improving the functionality of the device. Here we explore the possibility to supply heat from a nonelectronic source to produce electric power, and examine the efficiency as compared to the one of a conventional electronic two-terminal device.

The theoretical attempts to improve ζ [4–6] mostly pertain to setups which are time-reversal symmetric. This means that the matrix relating the fluxes (i.e., currents of particles and heat currents) to the thermodynamic driving forces (electric voltages and temperature differences) is symmetric [17, 18]. This matrix is composed of the Onsager coefficients, which in the *linear-response regime* are independent of the driving forces or the fluxes. An intriguing paper by Benenti *et al.* [19] raised the possibility of manipulating the performance of electronic thermoelectric devices by breaking time-reversal symmetry. In fact, invoking solely the Onsager reciprocity relations [17, 18, 20, 21] and the non-negativeness of the entropy production, Ref. 19 obtained the perplexing possibility of a two-terminal (2T) device operating at the Carnot efficiency while yielding a finite power. This result has been investigated in the literature of not only the quantum thermoelectricity, but also classical and quantum heat engines [22–24].

How can this claim be scrutinized? Time-reversal symmetry can be broken by magnetic fields. However, the linear-response Onsager coefficients of an electronic 2T device without interactions, i.e., with only elastic scattering, must be even functions of the magnetic field [25]. Thus, a prerequisite for this investigation is to find a realistic situation in which the asymmetry of the Onsager coefficients can be controlled. Here we respond to this challenge by adding inelastic processes. Our system allows for the inspection of the effect of a broken time-reversal symmetry in conjunction with inelastic processes, on the power-harvesting efficiency.

An effective two-terminal (E2T) setup can be constructed from an all-electronic three-terminal (3T) device [26–28] (or even from a multi-terminal electronic junction [29]). This proposal is based on the concept of probe terminals [30], whose temperatures and chemical potentials can be adjusted so as to cancel out the currents between those terminals and the device. In this way the multi-terminal setup is reduced to an E2T one. Though breaking time-reversal symmetry can enhance the efficiency of the E2T device, the unitarity of the 3T scattering matrix imposes strong bounds on the efficiency of the E2T, which are much lower than those of Ref. 19 [27, 28]. Adding more probe terminals can increase these bounds and

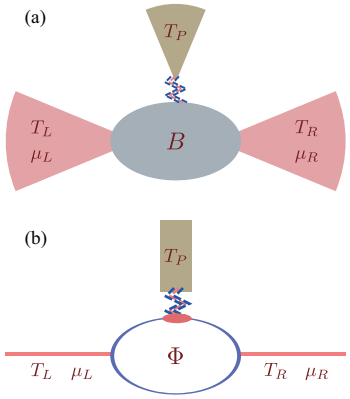

FIG. 1: (color online) Sketch (a) and simplified model (b) of a thermoelectric device, comprising two electronic terminals (held at chemical potentials μ_L and μ_R, and at temperatures T_L and T_R), and a thermal terminal held at a temperature T_P, with which the electrons exchange energy. The nanostructure [central (gray) disk], placed in a magnetic field B as in (a), is modeled by an Aharonov-Bohm ring threaded by a magnetic flux Φ as in (b). The electrons exchange energy with vibrational modes on a dot placed on the upper arm.

the resulting efficiency, but these still remain below those of Ref. 19 [29].

The matrix of the Onsager coefficients can be asymmetric when time-reversal symmetry is broken in the presence of inelastic interactions [31], or electron-phonon ones as considered here [32]. These interactions give rise to inelastic processes between the conduction electrons and the phonons, and those in turn imply the existence of thermal baths attached to the junction that exchange energy (but not particles) with the electronic system. Figure 1(a) illustrates a setup of this type [32]: a nanostructure is attached to two electronic baths held at chemical potentials μ_L and μ_R, and at temperatures T_L and T_R, and is coupled to a third, thermal bath, held at another temperature T_P. There are three independent currents flowing in this device, namely, the electric one between the electronic baths, the electronic heat current between them, and the phonon energy current. This setup becomes an E2T one with asymmetric Onsager coefficients when e.g., the driving forces are chosen so that the electronic heat current is blocked. In this way the device investigated in Ref. 19 is realized.

We find that while the entropy production of the 3T junction can vanish, that of the E2T junction cannot, as long as the magnetic field B is nonzero [33]. In other words, the E2T device is dissipative as long as $B \neq 0$, and its efficiency never reaches the Carnot bound. Though the argument of Ref. 19 is correct for the purely 2T setup, the upper bound on the efficiency is reduced. However, this upper bound increases with the strength of the electron-phonon interaction, and can exceed that found for the 3T all-electronic junctions [27].

The entropy production of the nanostructure in Fig. 1(a) is

$$\dot{S} = \frac{\langle \dot{E}_P \rangle}{T_P} + \frac{\langle \dot{E}_L \rangle - \mu_L \langle \dot{N}_L \rangle}{T_L} + \frac{\langle \dot{E}_R \rangle - \mu_R \langle \dot{N}_R \rangle}{T_R} \,, \quad (1)$$

where $-\langle \dot{E}_{L(R,P)} \rangle$ is the energy current out of the left electronic bath (right electronic bath, phonon bath) and $-\langle \dot{N}_{L(R)} \rangle$ is the particle current out of the left (right) electronic bath. The particle number conservation, $\langle \dot{N}_L + \dot{N}_R \rangle = 0$, uniquely identifies the charge current, $J_L = -e\langle \dot{N}_L \rangle = e\langle \dot{N}_R \rangle$ (e is the unit charge). In contrast, energy conservation, $\langle \dot{E}_P + \dot{E}_L + \dot{E}_R \rangle = 0$, does not yield unique identifications of the energy currents [34]. Choosing T_R as the reference, using the electronic heat current emerging from the left electronic bath [35], we have

$$J_L^Q = -\langle \dot{E}_L \rangle + \mu_L \langle \dot{N}_L \rangle \,, \quad (2)$$

and the heat current between the thermal terminal and the electrons, $J_P^Q = -\langle \dot{E}_P \rangle$, the entropy production becomes

$$T_R \dot{S} = V J_L + \delta t_{\rm el} J_L^Q + \delta t_{\rm e-p} J_P^Q \,. \quad (3)$$

The driving forces are the voltage drop, $V = (\mu_L - \mu_R)/e$, the (dimensionless) difference in the electronic temperatures, $\delta t_{\rm el} = 1 - T_R/T_L$, and the temperature difference between the phonon bath and the reference, $\delta t_{\rm e-p} = 1 - T_R/T_P$.

We consider the model displayed in Fig. 1(b), in which the nanostructure is an Aharonov-Bohm ring, threaded by a magnetic flux Φ. The ring is attached to two electronic reservoirs and carries a quantum dot on one of its arms; when the electrons are on the quantum dot they interact with the vibrational modes there. The latter are tightly coupled to a bath of phonons which fixes their population [36]. In our simplified model, the dot is replaced by a single localized electronic level of energy ϵ_0 and its vibrational modes are Einstein phonons of frequency ω_0; the electronic leads are assumed to contain free electron gases. With γ denoting the coupling energy of an electron with the vibrational modes, whose creation (annihilation) operators are $b^\dagger$ (b), and the creation (annihilation) operators of the electron on the localized level by $c_0^\dagger$ (c_0), the Hamiltonian (using $\hbar = 1$) is

$$\mathcal{H} = [\epsilon_0 + \gamma(b^\dagger + b)] c_0^\dagger c_0 + \omega_0 \left(b^\dagger b + \frac{1}{2} \right) + \sum_k \epsilon_k c_k^\dagger c_k + \sum_p \epsilon_p c_p^\dagger c_p$$
$$+ \sum_k (V_k c_k^\dagger c_0 + \text{H.c.}) + \sum_p (V_p c_p^\dagger c_0 + \text{H.c.}) + \sum_{k,p} (V_{kp} e^{i\Phi} c_k^\dagger c_p + \text{H.c.}) \,. \quad (4)$$

The operators that create (annihilate) a conduction electron in the left (right) lead, of energy $\epsilon_{k(p)}$, are $c^\dagger_{k(p)}$ ($c_{k(p)}$). The tunneling matrix elements between the localized level and the left (right) electronic lead are denoted by V_k (V_p). The lower arm of the ring in Fig. 1(b) connects the two leads with the tunneling matrix element V_{kp}; the magnetic flux Φ (in units of c/e) penetrating the ring is assigned to these elements. Since the magnetic field giving rise to the Aharonov-Bohm effect is usually small, one may neglect the tiny Zeeman effect on the spins of the conduction electrons.

The charge and heat currents flowing through the ring junction are found within the Keldysh formalism [37, 38]. The detailed calculation, carried out to the second order in the coupling γ, is summarized in Ref. 32. The charge current emerging from the left electronic lead is expressed in terms of the electrons' Green's functions,

$$J_L = -e\langle \dot{N}_L\rangle = -e\frac{d\langle\sum_k c^\dagger_k c_k\rangle}{dt} = -e\int\frac{d\omega}{2\pi}\mathcal{J}_L(\omega)\ , \quad (5)$$

where

$$\mathcal{J}_L(\omega) = \sum_k V_k[G_{k0}(\omega) - G_{0k}(\omega)]^< + \sum_{k,p} V_{kp}[e^{-i\Phi}G_{kp}(\omega) - e^{i\Phi}G_{pk}(\omega)]^< . \quad (6)$$

Here, $G^<_{ab}(\omega)$ is the lesser Keldysh Green's function [37], which is the Fourier transform of $G^<_{ab}(t,t') = i\langle c^\dagger_b(t')c_a(t)\rangle$, where a and b denote the relevant operators, [0, k, or p, see Eq. (4)]. The energy current emerging from the left electronic lead is given by $-\langle\dot{E}_L\rangle = d\langle\sum_k \epsilon_k c^\dagger_k c_k\rangle/dt$; it attains the same form as the charge current except for an extra factor ω in the integrand in Eq. (5) (and without the electron's charge e). The energy current of the thermal terminal can be obtained from $\langle\dot{E}_L + \dot{E}_R + \dot{E}_P\rangle = 0$.

Once the Green's functions are determined and inserted into the expressions for the currents, one expands the latter to linear order in the three driving forces, to obtain the Onsager coefficients. The result can be presented in a matrix form,

$$\begin{bmatrix} J_L \\ J^Q_L \\ J^Q_P \end{bmatrix} = \mathcal{M}\begin{bmatrix} V \\ \delta t_{\rm el} \\ \delta t_{\rm e-p} \end{bmatrix}\ , \quad (7)$$

where $\mathcal{M}$ is the 3×3 matrix of the Onsager coefficients of the device; its elements depend on the choice of the driving forces [34]. Reference 32 presents the elements of the matrix $\mathcal{M}$ for an arbitrary ring junction (i.e., that does not possess any special spatial symmetries). All off-diagonal elements of $\mathcal{M}$ contain terms odd in the magnetic flux (which obey the Onsager reciprocity relations). Remarkably enough, *all* these odd terms arise from inelastic processes in which the charge carriers exchange energy (ω_0) with the vibrational modes. All elements of $\mathcal{M}$ also contain terms even in the flux; these arise from elastic as well as inelastic processes of the transport electrons [32]. In the absence of the coupling of the electrons with the vibrational modes, the Onsager coefficients would be even in the flux and $\mathcal{M}$ would be symmetric.

For a spatially-symmetric junction, the matrix $\mathcal{M}$ is [32]

$$\mathcal{M} = \begin{bmatrix} G & \mathcal{S}G & 0 \\ G\mathcal{S} & \kappa_0 & -P(1+a) \\ 0 & -P(1-a) & 2P \end{bmatrix}\ , \quad (8)$$

where $a = \tau_0\sin\Phi$, which is odd in the magnetic field, and τ_0 is the transmission of the lower arm of the ring (assumed for simplicity to be energy independent). In Eq. (8), G is the electric conductance and $\mathcal{S}$ is the Seebeck coefficient; κ_0 is the "bare" thermal conductance of the electrons, i.e., for $\gamma = 0$, the heat conductance of the electrons is $\kappa_0 - G\mathcal{S}^2$. These three coefficients, for the ring geometry of Fig. 1(b), are functions of $\cos\Phi$ [32]. The other three elements in $\mathcal{M}$ are due to inelastic processes (and vanish at zero temperature),

$$P = \omega_0^2\int\frac{d\omega}{\pi}\mathcal{T}_{\rm p}(\omega,\Phi)\ , \quad (9)$$

where $\mathcal{T}_{\rm p}$ is the transmission of the inelastic processes,

$$\mathcal{T}_{\rm p}(\omega,\Phi) = \frac{\beta_R}{e^{\beta_R\omega_0}-1}f(\omega_-)[1-f(\omega_+)]c(\omega,\Phi)\ . \quad (10)$$

Here, $f(\omega) = (\exp[\beta_R(\omega-\mu_R)]+1)^{-1}$ (recall that temperatures and chemical potentials are measured with respect to the right electronic lead), $\omega_\pm = \omega \pm \omega_0/2$,

$$c(\omega,\Phi) = \frac{\gamma^2}{4}\Gamma(\omega_-)\Gamma(\omega_+)|\mathcal{G}^a_{00}(\omega_-,\Phi)\mathcal{G}^a_{00}(\omega_+,\Phi)|^2\ , \quad (11)$$

Γ represents the width of the resonance on the dot due to the coupling with the electronic leads, and $\mathcal{G}^a_{00}$ is the advanced Green's function there in the absence of the coupling with the vibrations; $2P \geq 0$ is the heat conductance of the phonons, proportional to γ^2, the electron-phonon coupling squared [32].

Inserting the explicit expressions for the currents [Eqs. (7) and (8)] into Eq. (3), one finds that the entropy production of the 3T device is non-negative, $\dot{S} \geq 0$, for

$$\kappa_0 - G\mathcal{S}^2 - P/2 \geq 0\ ,\ \text{i.e.,}\ 2\kappa_0/P \geq 1+\zeta\ , \quad (12)$$

where $\zeta = G\mathcal{S}^2/(\kappa_0 - G\mathcal{S}^2)$ is the figure of merit of the conventional electronic 2T device [see e.g., Ref. 4].

The electronic heat current J^Q_L can be blocked by choosing

$$\delta t_{\rm el} = -\frac{1}{\kappa_0}[G\mathcal{S}V - P(1+a)\delta t_{\rm e-p}]\ . \quad (13)$$

The setup then becomes an E2T, in which electric power is produced at the expense of thermal power from the phonon bath. The matrix of the Onsager coefficients pertaining to this configuration is not symmetric, that is, the off-diagonal elements are not even in the magnetic field [39],

$$\begin{bmatrix} J_L \\ J^Q_P \end{bmatrix} = \begin{bmatrix} \frac{G}{1+\zeta} & \frac{PG\mathcal{S}}{\kappa_0}(1+a) \\ \frac{PG\mathcal{S}}{\kappa_0}(1-a) & \frac{P^2}{\kappa_0}(\zeta_{\rm max}+a^2) \end{bmatrix}\begin{bmatrix} V \\ \delta t_{\rm e-p} \end{bmatrix}\ , \quad (14)$$

where $\zeta_{\rm max} = -1 + 2\kappa_0/P$ is the upper bound on ζ, imposed by the condition (12). The entropy production in the E2T setup described by Eq. (14), which is proportional to $J_L V + J_P^Q \delta t_{\rm e-p}$, is non-negative for

$$2\kappa_0/P + a^2 \geq 1 + \zeta \, . \tag{15}$$

The equality in Eq. (15) is what Benenti *et al.* [19] used in discussing the possibility to achieve the Carnot efficiency at a finite power. However, taking account of the 3T setup, which is the background of the E2T device, implies that the stricter inequality (12) must hold, and that the equality of Eq. (15) is not achievable for a nonzero $a = \tau_0 \sin\Phi$. This means that as long as the magnetic field [33] is finite, the entropy production of the E2T junction cannot reach the reversible limit. Thus, the Carnot bound is not reached, although the symmetry of the E2T Onsager coefficients is broken.

The efficiency for producing electric power at the expense of the phonons' energy current, i.e., $V \leq 0$ and $\delta t_{\rm e-p} \geq 0$, is

$$\eta = -V J_L / J_P^Q \, . \tag{16}$$

The electric power $|V J_L|$ is maximal at $V_{\rm MP} = -\delta t_{\rm e-p}(1+\zeta)(1+a)P\mathcal{S}/(2\kappa_0)$, and then the efficiency at the maximal power is

$$\eta(V_{\rm MP}) = \eta_{\rm rev} \frac{(1+a)^2\zeta/4}{\zeta_{\rm max} + a^2 - (1-a^2)\zeta/2} \, , \tag{17}$$

where $\eta_{\rm rev} = \delta t_{\rm e-p}$ is the Carnot efficiency, i.e., $\eta(V_{\rm MP}; \zeta = \zeta_{\rm max}, a = 0) = \eta_{\rm rev}/2$. Figure 2 displays $\eta(V_{\rm MP})$ of the E2T device as a function of the symmetry breaking parameter a for several values of $\zeta \leq \zeta_{\rm max} = 10$. The horizontal line shows the maximal electronic 2T efficiency at maximal power, $\eta_{\rm max}(V_{\rm MP})/\eta_{\rm rev} = \zeta_{\rm max}/(4 + 2\zeta_{\rm max})$. Interestingly, all the graphs have a minimum, $\eta(V_{\rm MP}) = 0$, at $a = -1$ (destructive interference on the Aharonov-Bohm ring), and a maximum at $a = 1$ for $\zeta < \zeta_{\rm max} - 1$ or at $a = (2\zeta_{\rm max} - \zeta)/(2 + \zeta)$ for $\zeta > \zeta_{\rm max} - 1$. This maximal value reaches the Carnot efficiency when $\zeta = \zeta_{\rm max} \to \infty$, but then the power vanishes. Remarkably enough, $\eta(V_{\rm MP})$ of the E2T is improved as the asymmetry in the Onsager coefficients is increased (except for a narrow region near $\zeta_{\rm max}$) and as $\zeta_{\rm max} = 2\kappa_0/P - 1$ increases; at large enough ζ, the E2T device is more efficient than the 2T electronic one and is significantly higher than $\eta_{\rm max}(V_{\rm MP})/\eta_{\rm rev} = 4/7$, found in Ref. 27 for $a = 1/7$.

Another quantity of interest is the maximal value of the efficiency Eq. (16), reached when the voltage is

$$\frac{V_{\rm ME}}{\delta t_{\rm e-p}} = \frac{P(\zeta_{\rm max} + a^2)}{G\mathcal{S}(1-a)} \left(\left[1 - \frac{(1-a^2)\zeta}{\zeta_{\rm max} + a^2} \right]^{\frac{1}{2}} - 1 \right) . \tag{18}$$

This efficiency can be written in the form

$$\eta(V_{\rm ME}) = \eta_{\rm rev} [\sqrt{1+\widetilde{\zeta}} - 1]/[\sqrt{1+\widetilde{\zeta}} + 1] \, , \tag{19}$$

with the new figure of merit of the E2T device,

$$\widetilde{\zeta} = \zeta \frac{(1-a^2)^2/(\zeta_{\rm max} + a^2)}{\left(\left[1 - (1-a^2)\zeta/(\zeta_{\rm max} + a^2) \right]^{\frac{1}{2}} - a \right)^2} \, . \tag{20}$$

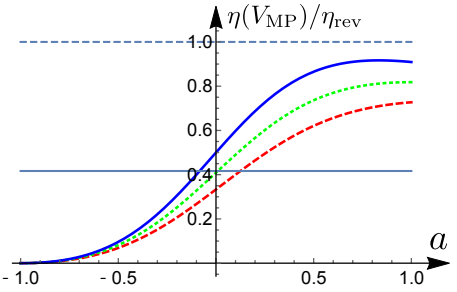

FIG. 2: (color online) The efficiency at maximal power of the E2T device (scaled by the Carnot efficiency $\eta_{\rm rev}$), Eq. (17), as a function of the asymmetry parameter a, for $\zeta_{\rm max} = 10$; $\zeta = 8$ [the dashed (red) curve], 9 [the dotted (green) curve], and 10 [the thick (blue) line]. The horizontal line is $\eta(V_{\rm MP}, \zeta = \zeta_{\rm max})/\eta_{\rm rev}$ of the 2T junction.

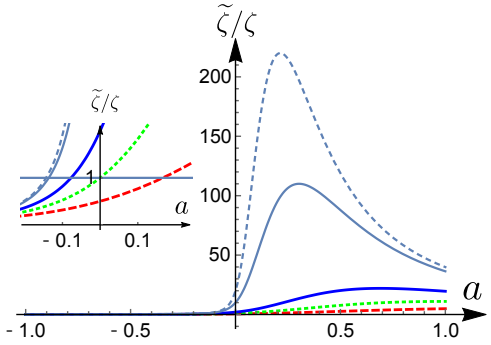

FIG. 3: (color online) The E2T figure of merit $\widetilde{\zeta}$, Eq. (20) (scaled by the 2T one, ζ), as a function of a, for $\zeta_{\rm max} = 10$; $\zeta = 8$ [the dashed (red) curve], 9 [the dotted (green) curve], 9.5 [the thick (blue) line], 9.9 [the thin (black) curve], and 9.95 [the thin dashed (black) curve]. Inset: The range where $\widetilde{\zeta}/\zeta$ crosses 1.

We plot $\widetilde{\zeta}/\zeta$ as a function of a in Fig. 3, which shows that $\widetilde{\zeta}$ can significantly exceed ζ of the 2T electronic device. As for $\eta(V_{\rm MP})$, $\widetilde{\zeta}$ has a maximum at a certain positive a, which grows and moves to smaller values of a as ζ increases. The inset displays the region around $\zeta = \widetilde{\zeta}$. As seen, $\widetilde{\zeta}$ increasingly exceeds ζ, making the E2T device better than the electronic 2T one.

In conclusion, we demonstrated that for our effective two-terminal quantum device, breaking the time-reversal symmetry yields efficiencies which can approach the Carnot efficiency, but are always lower than it. It is not sufficient to consider only the effective 2×2 Onsager matrix. Including the restrictions from the entropy production of the underlying three-terminal device one finds that the Carnot efficiency cannot be reached with a nonvanishing power. The efficiency of our device can exceed that in the 3T all-electronic device [27]. We conjecture that similar restrictions apply to other effective two-terminal devices, but a general proof remains a challenge for future work. An experimental realization of our model could test the predictions concerning the advantages of phonon heat source over an electronic one for producing elec-

tricity, in particular under the effect of a magnetic field.

Useful comments given by G. Benenti are gratefully acknowledged. O. E. W. and A. A. acknowledge support from the infrastructure program of the Israel Ministry of Science and Technology under Contract No. 3-11173 and the kind hospitality of the Institute of Industrial Science at the University of Tokyo. K. Y. is supported by the Advanced Leading Graduate Course for Photon Science (ALPS), the University of Tokyo as well as by a Grant-in-Aid for Japan Society for the Promotion of Science (JSPS) Fellows (Grant No.16J11542). N. H. is supported by Kakenhi Grants No. 15K05200, No. 15K05207, and No. 26400409 from the Japan Society for the Promotion of Science.

* Electronic address: kaoru3@iis.u-tokyo.ac.jp
† Electronic address: oraentin@bgu.ac.il
‡ Electronic address: hatano@iis.u-tokyo.ac.jp

[1] M. S. Dresselhaus, G. Chen, M. Y. Tang. R. G. Yang, H. Lee, D. Z. Wang, Z. F. Ren, J.-P. Fleurial, and P. Gogna, *New Directions for Low-Dimensional Thermoelectric Materials*, Adv. Mater. **19**, 1043 (2007).

[2] C. Vineis, A. Shakouri, A. Majumdar, and M. G. Kanatzidis, *Nanostructured Thermoelectrics: Big Efficiency Gains from Small Features*, Adv. Mater. **22**, 3970 (2010).

[3] A. Shakouri, *Recent Developments in Semiconductor Thermoelectric Physics and Materials*, Annu. Rev. Mater. Res. **41**, 399 (2011).

[4] J. D. Mahan and J. O. Sofo, *The best thermoelectric*, Proc. Natl. Acad. Sci. U.S.A. **93**, 7436 (1996).

[5] T. E. Humphrey, R. Newbury, R. P. Taylor, and H. Linke, *Reversible Quantum Brownian Heat Engines for Electrons*, Phys. Rev. Lett. **89**, 116801 (2002).

[6] T. E. Humphrey and H. Linke, *Reversible Thermoelectric Nanomaterials*, Phys. Rev. Lett. **94**, 096601 (2005).

[7] R. S. Whitney, *Most Efficient Quantum Thermoelectric at Finite Power Output*, Phys. Rev. Lett. **112**, 130601 (2014).

[8] M. Polettini, G. Verley, and M. Esposito, *Efficiency Statistics at All Times: Carnot Limit at Finite Power*, Phys. Rev. Lett. **114**, 050601 (2015).

[9] K. Proesmans, C. Driesen, B. Cleuren, and C. Van den Broeck, *Efficiency of single-particle engines*, Phys. Rev. E **92**, 032105 (2015).

[10] M. Esposito, M. A. Ochoa, and M. Galperin, *Efficiency fluctuations in quantum thermoelectric devices*, Phys. Rev. B **91**, 115417 (2015).

[11] Fluctuations of the efficiency were studied also in time-reversal-broken systems, see J.-H. Jiang, B. K. Agarwalla, and D. Segal, *Efficiency Statistics and Bounds for Systems with Broken Time-Reversal Symmetry*, Phys. Rev. Lett. **115**, 040601 (2015); B. K. Agarwalla, J.-H. Jiang, and D. Segal, *Full counting statistics of vibrationally assisted electronic conduction: Transport and fluctuations of thermoelectric efficiency*, Phys. Rev. B **92**, 245418 (2015).

[12] F. Mazza, R. Bosisio, G. Benenti, V. Giovannetti, R. Fazio and F. Taddei, *Thermoelectric efficiency of three-terminal quantum thermal machines*, New J. Phys. **16**, 085001 (2014).

[13] B. Szukiewicz, U. Eckern, and K. I. Wysokiński, *Optimisation of a three-terminal nonlinear heat nano-engine*, New J. Phys. **18**, 023050 (2016).

[14] H. Thierschmann, R. Sánchez, B. Sothmann, F. Arnold, C. Heyn, W. Hansen, H. Buhmann, and L. W. Molenkamp, *Three-terminal energy harvester with coupled quantum dots*, Nature Nanotechnology **10**, 854 (2015).

[15] H. Thierschmann, R. Sánchez, B. Sothmann, H. Buhmann, and L. W. Molenkamp, *Thermoelectrics with Coulomb coupled Quantum Dots*, arXiv:1603.08900.

[16] F. Mazza, S. Valentini, R. Bosisio, G. Benenti, V. Giovannetti, R. Fazio and F. Taddei, *Separation of heat and charge currents for boosted thermoelectric conversion*, Phys. Rev. B **91**, 245435 (2015).

[17] L. Onsager, *Reciprocal Relations in Irreversible Processes*, Phys. Rev. **38**, 2265 (1931).

[18] H. B. G. Casimir, *On Onsager's Principle of Microscopic Reversibility*, Rev. Mod. Phys. **17**, 343 (1945).

[19] G. Benenti, K. Saito, and G. Casati, *Thermodynamic Bounds on Efficiency for Systems with Broken Time-Reversal Symmetry*, Phys. Rev. Lett. **106**, 230602 (2011).

[20] For a recent experimental verification of the Onsager reciprocity relations in thermoelectric quantum transport, see J. Matthews, F. Battista, D. Sánchez, P. Samuelsson, and H. Linke, *Experimental verification of reciprocity relations in quantum thermoelectric transport*, Phys. Rev. B **90**, 165428 (2014).

[21] For a generalization of the Onsager relations to include coherent electron systems under adiabatic ac driving, see M. F. Ludovico and L. Arrachea, *Pumping charge with ac magnetic fluxes and the dynamical breakdown of Onsager symmetry*, Phys. Rev. B **87**, 115408 (2013); M. F. Ludovico, F. Battista, F. von Oppen, and L. Arrachea, *Adiabatic response and quantum thermoelectrics for ac-driven quantum systems*, Phys. Rev. B **93**, 075136 (2016).

[22] K. Brandner, K. Saito, and U. Seifert, *Thermodynamics of Micro- and Nano-Systems Driven by Periodic Temperature Variations*, Phys. Rev. X **5**, 031019 (2015).

[23] K. Proesmans, C. Van den Broeck, *Onsager coefficients in periodically driven systems* , Phys. Rev. Lett. **115**, 090601 (2015).

[24] N. Shiraishi, K. Saito, and H. Tasaki, *Universal trade-off relation between power and efficiency for heat engines*, arXiv:1605.00356 (2016).

[25] M. Büttiker, *Symmetry of electrical conduction*, IBM J. Res. Dev. **32**, 317 (1988).

[26] K. Saito, G. Benenti, G. Casati, and T. Prosen, *Thermopower with broken time-reversal symmetry*, Phys. Rev. B **84**, 201306(R) (2011).

[27] K. Brandner, K. Saito, and U. Seifert, *Strong Bounds on Onsager Coefficients and Efficiency for Three-Terminal Thermoelectric Transport in a Magnetic Field*, Phys. Rev. Lett. **110**, 070603 (2013).

[28] V. Balachandran, G. Benenti and G. Casati, *Efficiency of three-terminal thermoelectric transport under broken time-reversal symmetry*, Phys. Rev. B **87**, 165419 (2013).

[29] K. Brandner and U. Seifert, *Multi-terminal thermoelectric transport in a magnetic field: bounds on Onsager coefficients and efficiency*, New J. Phys. **15**, 105003 (2013); *Bound on thermoelectric power in a magnetic field within linear response*, Phys. Rev. E **91**, 012121 (2015).

[30] M. Büttiker, *Role of quantum coherence in series resistors*, Phys. Rev. B **33**, 3020 (1986).

[31] D. Sánchez and L. Serra, *Thermoelectric transport of mesoscopic conductors coupled to voltage and thermal probes*, Phys. Rev. B **84**, 201307(R) (2011).

[32] O. Entin-Wohlman and A. Aharony, *Three-terminal thermoelectric transport under broken time-reversal symmetry*, Phys.

Rev. B **85**, 085401 (2012).

[33] The magnetic field in the model of Ref. 32 enters the Onsager matrix as a trigonometric function of the flux Φ; strictly speaking, the entropy production can then vanish whenever $\sin\Phi$ vanishes. To avoid this complexity, the discussion is confined to small fields.

[34] Indeed, the driving forces used here differ from those used in Ref. 32. See also K. Yamamoto, *Thermodynamics of mesoscopic quantum systems*, Master Thesis, University of Tokyo (2015); arXiv:1504.05493.

[35] K. Yamamoto and N. Hatano, *Thermodynamics of the mesoscopic thermoelectric heat engine beyond the linear-response regime*, Phys. Rev. E **92**, 042165 (2015).

[36] O. Entin-Wohlman, Y. Imry, and A. Aharony, *Transport through molecular junctions with a nonequilibrium phonon population*, Phys. Rev. B **81**, 113408 (2010).

[37] H. J. W. Haug and A.-P. Jauho, *Quantum Kinetics in Transport and Optics of Semiconductors*, Springer Series in Solid-State Sciences, Vol. 123 (Springer-Verlag, Berlin, 2008).

[38] Note that since the junction comprises a thermal terminal that gives rise inelastic scattering processes, the Büttiker-Landauer scattering-matrix formalism used to study all-electronic junctions [26–29] is not applicable for our model.

[39] Other possible configurations, like the "cooling by heating" scenario [see B. Cleuren, B. Rutten, and C. Van den Broeck, *Cooling by Heating: Refrigeration Powered by Photons*, Phys. Rev. Lett. **108**, 120603 (2012)], will be investigated elsewhere.